The Transcription Factor 7-Like 2-Peroxisome Proliferator-Activated Receptor Gamma Coactivator-1 Alpha Axis Connects Mitochondrial Biogenesis and Metabolic Shift with Stem Cell Commitment to Hepatic Differentiation

Wanet, Anaïs; Caruso, Marino; Domelevo Entfellner, Jean Baka; Najar, Mehdi; Fattaccioli, Antoine; Demazy, Catherine; Evraerts, Jonathan; El-Kehdy, Hoda; Pourcher, Guillaume; Sokal, Etienne; Arnould, Thierry; Tiffin, Nicki; Najimi, Mustapha; Renard, Patricia

Published in:
Stem Cells

DOI:
10.1002/stem.2688

Publication date:
2017

Document Version
Publisher's PDF, also known as Version of record

STEM CELLS®

TISSUE-SPECIFIC STEM CELLS

The Transcription Factor 7-Like 2–Peroxisome Proliferator-Activated Receptor Gamma Coactivator-1 Alpha Axis Connects Mitochondrial Biogenesis and Metabolic Shift with Stem Cell Commitment to Hepatic Differentiation

ANAÏS WANET,[a] MARINO CARUSO,[a] JEAN-BAKA DOMELEVO ENTFELLNER,[b] MEHDI NAJAR,[c] ANTOINE FATTACCIOLI,[a] CATHERINE DEMAZY,[a] JONATHAN EVRAERTS,[d] HODA EL-KEHDY,[d] GUILLAUME POURCHER,[e] ETIENNE SOKAL,[d] THIERRY ARNOULD,[a] NICKI TIFFIN,[b] MUSTAPHA NAJIMI,[d] PATRICIA RENARD[a]

Key Words. Hepatic differentiation • Stem cells • Mitochondria • Oxidative phosphorylation • Wnt/β-catenin

ABSTRACT

Increasing evidence supports that modifications in the mitochondrial content, oxidative phosphorylation (OXPHOS) activity, and cell metabolism influence the fate of stem cells. However, the regulators involved in the crosstalk between mitochondria and stem cell fate remains poorly characterized. Here, we identified a transcriptional regulatory axis, composed of transcription factor 7-like 2 (*TCF7L2*) (a downstream effector of the Wnt/β-catenin pathway, repressed during differentiation) and peroxisome proliferator-activated receptor gamma coactivator-1 alpha (*PGC-1α*) (the master regulator of mitochondrial biogenesis, induced during differentiation), coupling the loss of pluripotency and early commitment to differentiation, to the initiation of mitochondrial biogenesis and metabolic shift toward OXPHOS. PGC-1α induction during differentiation is required for both mitochondrial biogenesis and commitment to the hepatocytic lineage, and TCF7L2 repression is sufficient to increase PGC-1α expression, mitochondrial biogenesis and OXPHOS activity. We further demonstrate that OXPHOS activity is required for the differentiation toward the hepatocytic lineage, thus providing evidence that bi-directional interactions control stem cell differentiation and mitochondrial abundance and activity. STEM CELLS *2017;35:2184–2197*

SIGNIFICANCE STATEMENT

Mitochondria, which represent the major source of energy and power for the cells, are increasingly recognized as major regulators of stem cells. In this study, we show that increasing the content and activity of mitochondria is essential for stem cell differentiation into hepatocytes. We identified a regulatory axis that couples the loss of pluripotency and commitment to differentiation to the increase of mitochondria abundance and activity. In turn, mitochondrial activity further supports the differentiation process. By better deciphering the interplay between mitochondria and stem cell differentiation, these findings could benefit the development of stem-cell based therapeutics and regenerative medicine.

INTRODUCTION

Mitochondrial biogenesis and metabolism recently emerged as critical modulators of stemness properties and differentiation programs [1]. Inhibiting mitochondrial biogenesis or function prevents or disturbs the differentiation of stem cells into multiple lineages [2] and facilitates the reprogramming of somatic cells into induced pluripotent stem cells [3]. These data support a crucial role for mitochondria and energy metabolism in the regulation of pluripotency and differentiation-related pathways. However, the molecular regulators involved in this crosstalk between pluripotency and differentiation on the one hand, and mitochondrial biogenesis and metabolism on the other hand, are still poorly characterized.

Conceptually, one can distinguish upstream and downstream regulators of the interplay

[a]Laboratory of Biochemistry and Cell Biology (URBC), NAmur Research Institute for LIfe Sciences (NARILIS), University of Namur (UNamur), Namur, Belgium; [b]South African National Bioinformatics Institute (SANBI)/Medical Research Council of South Africa Bioinformatics Unit, University of the Western Cape, Bellville, South Africa; [c]Laboratory of Clinical Cell Therapy, Institut Jules Bordet, Université Libre de Bruxelles (ULB), Brussels, Belgium; [d]Laboratory of Pediatric Hepatology and Cell Therapy, Université Catholique de Louvain, Institut de Recherche Clinique et Expérimentale (IREC), Brussels, Belgium; [e]Department of Digestive Diseases, Institut Mutualiste Montsouris, Paris Descartes University, Paris, France

Correspondence: Patricia Renard, Ph.D., Laboratory of Biochemistry and Cell Biology (URBC), University of Namur, rue de Bruxelles 61, 5000 Namur, Belgium. Telephone: +320-81-724-128; Fax: +320-81-724-135; e-mail: patsy.renard@unamur.be

Received September 18, 2017; accepted for publication July 15, 2017; first published online in STEM CELLS *EXPRESS* August 10, 2017.

http://dx.doi.org/10.1002/stem.2688

between mitochondrial biogenesis and stem cell differentiation. The upstream regulators of the interplay could be defined as the regulators involved in pluripotency and/or differentiation pathways responsible for the control of mitochondrial biogenesis and metabolism. The downstream regulators on the other hand, could be defined as the regulators of cell differentiation that are activated following the induction of mitochondrial biogenesis and metabolic shift. An example of upstream regulator is the transcription factor hypoxia inducible factor 1 alpha (HIF-1α). In embryonic stem cells (ESCs), HIF-1α positively regulates the expression of pluripotency genes while inhibiting the expression of peroxisome proliferator-activated receptor gamma coactivator-1 alpha (*PGC-1α*) [4], the master regulator of mitochondrial biogenesis [5, 6]. Therefore, HIF-1α maintains pluripotency while inhibiting mitochondrial biogenesis in ESCs [4]. An example of downstream effectors are the mitochondrial reactive oxygen species (ROS) produced during the adipogenic differentiation of bone marrow mesenchymal stem cells (BM-MSCs), which are required for the induction of the *PPARγ*, a master regulator of adipogenesis [7]. The question whether those regulators are involved in the crosstalk between mitochondrial biogenesis and stem cell differentiation in different models remains to be determined. It is likely that stem cell and lineage-specificities exist, and that other molecular actors may act together and/or independently of them in that process.

In this study, we investigated the crosstalk between mitochondrial biogenesis and the hepatocytic differentiation of BM-MSCs. We found that the mitochondrial biogenesis and metabolic shift toward oxidative phosphorylation (OXPHOS) occur within the first days of hepatocytic differentiation and overlap the loss of genes belonging to multipotency-related pathways. Bioinformatics analyses of transcriptomics data collected during the early steps of the differentiation process enabled us to identify multiple putative co-regulators of mitochondrial biogenesis and cell differentiation, among which is *PGC-1α*. We found that *PGC-1α* is required both for the induction of mitochondrial biogenesis and for the proper differentiation of BM-MSCs into hepatocyte-like cells. To understand how *PGC-1α* expression is induced during hepatocytic differentiation, we analyzed the expression of predicted regulators of *PGC-1α*. Among them is transcription factor 7-like 2 (*TCF7L2*), a downstream effector of the Wnt/β-catenin signaling pathway. We evidenced that TCF7L2 controls *PGC-1α* expression, mitochondrial biogenesis, and OXPHOS activity in BM-MSCs, supporting the hypothesis that *TCF7L2* repression during hepatocytic differentiation initiates *PGC-1α* induction, mitochondrial biogenesis, and metabolic shift.

Materials and Methods

Cell Culture and Differentiation

Cultures of human BM-MSCs were established as described previously [8] after informed consent from healthy donors and the approval of the local ethics committee of the Jules Bordet Institute (Belgium). For all studies, at least three independent replicates using cells isolated from different donors were performed. All experiments were performed using cells from passages 4–7.

BM-MSCs were expanded in 1 g/l glucose Dulbecco's Modified Eagle Medium supplemented with 1% penicillin–streptomycin (PS) mixture (Life Technologies, Carlsbad, CA, now part of Thermo Fisher (https://www.thermofisher.com/us/en/home/brands/life-technologies.html)) and 10% fetal bovine serum (FBS, PAA/GE Healthcare, Chicago, IL, http://www3.gehealthcare.com) ("Exp" condition). Before the hepatocytic induction, BM-MSCs were seeded on type-1 collagen (BD Biosciences, San Jose, CA, http://www.bdbiosciences.com)-coated dishes and expanded till 95% confluency ("day 0") (illustrated on Fig. 2). Hepatocytic induction was carried out by incubating BM-MSCs in Iscove's Modified Dulbecco's Medium (IMDM, Life Technologies) containing 1% PS mixture and supplemented with 20 ng/ml epidermal growth factor (PeproTech, Rocky Hill, NJ, https://www.peprotech.com) and 10 ng/ml basic-fibroblast growth factor (FGF-2, PeproTech) for 48 hours and then with 10 ng/ml FGF-2, 20 ng/ml hepatocyte growth factor (PeproTech), 0.61 mg/ml nicotinamide (Sigma-Aldrich, Saint-Louis, MO, https://www.sigmaaldrich.com), and insulin–transferrin–selenium (ITS) mixture 1X (Life Technologies) for 10 days. Cells were then treated with a hepatocytic maturation cocktail containing 20 ng/ml oncostatin M (PeproTech), 1 μM dexamethasone (Sigma-Aldrich) and ITS for 10 days. Undifferentiated BM-MSCs were maintained in IMDM supplemented with 1% FBS and 1% PS. For experiments involving OXPHOS inhibitors, cells were differentiated or left undifferentiated in the presence of 1 μM myxothiazol (Sigma-Aldrich), 5 μM antimycin A (Sigma-Aldrich), 1 μM oligomycin (Sigma-Aldrich), or the corresponding vehicles (1:2,000 dimethyl sulfoxide for myxothiazol and 1:2,000 ethanol for antimycin A and oligomycin) throughout the differentiation time course.

Lentiviral Vectors Production and Lentiviral Transduction

Lentiviral vectors were produced in HEK293T cells following transfection of envelope plasmid (pCMV-VSV-G, Addgene, Cambridge, MA, https://www.addgene.org, #8454), packaging plasmid (psPAX2, Addgene #12260), and expression plasmid [pLKO.1 puro backbone containing the non mammalian shRNA control (shNT, SHC002) or shRNA against PGC-1α (TRCN0000001165) or TCF7L2 (TRCN0000061897) (Sigma-Aldrich)]. Lentiviral vectors were titrated using the quantitative polymerase chain reaction (qPCR) Lentivirus Titration kit (Applied Biological Material, Vancouver, Canada, https://www.abmgood.com), according to the manufacturer's instructions. BM-MSCs at 60% confluency were transduced in 25 cm^2 flasks with 20×10^6 millions of lentiviral particles in the presence of 60 μg/ml protamine sulphate (Sigma-Aldrich). Transduced cells were selected with puromycin 1 μg/ml for 4–6 days and left without puromycin at least 2 days before experiments.

Massive Analysis of cDNA Ends Analysis

Total RNA was isolated using the RNeasy Mini kit and Qiacube (Qiagen, Hilden, Germany, https://www.qiagen.com). For each condition, equal amounts of RNA isolated from five independent donor cell batches were pooled and submitted to massive analysis of cDNA ends (GenXPro, Frankfurt, Germany, http://genxpro.net). Transcript per million normalization and tests for differential expression of mapped reads were performed in the statistical programming language R (www.rproject.org/) using the DEGexp function of the DEGseq package [9], after replacing the "0" counts by the arbitrary "0.5" value. Data were deposited in NCBI's Gene Expression Omnibus [10] and are accessible through GEO Series accession number GSE75184. Genes were considered as differentially expressed if upregulated or downregulated with a $p < .05$ or

with a $p < .25$ concomitantly with a |log2 fold-change| > 0.3785 (i.e., with fold changes >1.3 or < 0.769) (Supporting Information Table S1). Since the *p*-value calculation relies on the number of reads obtained for each gene, this procedure enabled us to take into account genes with low mRNA levels, such as many transcriptional regulators and co-regulators. Thus, genes considered as differentially expressed in this study include (a) genes that are statistically differentially expressed ($p < .05$), whatever the magnitude of the fold-change is and (b) genes that display a fold-change greater than the indicated threshold (>1.3 or < 0.769), although with a reduced statistical confidence ($p < .25$). Importantly, only differentially expressed genes (DEGs) displaying a simultaneous up- or downregulation in the three comparisons (differentiation vs. expansion, differentiation vs. day 0, and differentiation vs. undifferentiation within the same time point) were considered in our analyses (Fig. 2). The requirement for a gene to be selected in the three comparisons at the same time point enabled us to select the changes due to the cell differentiation per se and not the expression changes due to the prolonged in vitro culture without serum (comparisons vs. undifferentiated cells) or change in confluency (comparisons vs. expansion condition) or basal medium (comparisons vs. expansion or vs. day 0).

Pathway and Gene Ontology Analyses

Data were analyzed using the QIAGEN's Ingenuity Pathway Analysis suite (IPA, QIAGEN, www.qiagen.com/ingenuity). Gene ontology (GO)-TERMS annotations were analyzed using DAVID Bioinformatics Resources [11].

Identification of Predicted Co-Regulators of Mitochondrial Biogenesis and Stem Cell Commitment to Differentiation

Biological process-, cell component-, and molecular function-associated GO terms were retrieved for DEGs at day 5 of differentiation. DEGs were then sorted based on their GO annotations: one set was established with genes containing annotations related to mitochondria ("Mitochondria dataset," Supporting Information Table S2), another one with genes containing annotations related to (mesenchymal) stem cells or differentiation ("Stem-diff dataset," Supporting Information Table S3). The "upstream analysis" function of IPA was used to identify the putative regulators of these two lists of DEGs (Supporting Information Tables S4, S5). This function, which relies on a database containing the expected effects between transcriptional regulators and their target genes, retrieves the transcriptional regulators that are putatively involved in the differential expression of a list of genes. It also predicts whether these regulators are likely activated or inhibited, based on the expression value of their targets.

Real-Time Reverse Transcriptase-qPCR Analysis

RNA extraction, cDNA synthesis, and qPCR were performed as described previously [12] using the following primers: *a1AT* (a-1-antitrypsin) F: GGGTCAACTGGGCATCACTAA R: CCCTTTCT CGTCGATGGTCA; *CPS1* (carbamoyl phosphate synthetase 1) F: TCCTGATAGGCATCCAGCAATC R: AGGGACATTGTTGGCGTTGA; *PGC-1α* (peroxisome proliferator-activated receptor gamma, coactivator 1 alpha) F: TCCTTTCTCTCGCCCAACACGATCT R: GC ATCCGACAGGACAAACAGTGGA; glutamine synthetase (*GLUL*) F: CGCCGAGATGAGAAAGTTGT R: AAGCATGGCAGAGTGGGTAA; DNA polymerase gamma (*POLG*) F: TGGCCTTGCAGATCACCAA CCT R: TCCTTCCTGAGGCACCGGTCAA; *POLG2* (DNA Polymerase Gamma 2, Accessory Subunit) F: TCGACTCCAGTGGTGGAGAAA R: TTCCTTTCCGGCCTTCTTCAT; *POLRMT* (RNA Polymerase, Mitochondrial) F: GTGTACGGGGTCACGCGCTA R: CCGAGAACA TCTCCTGTAGACTCTT; *PPIE* (Peptidyl-prolyl cis-trans isomerase E) F: CCGCTCTTGACCCTGCATAT R: TCCAAGCAGACCCTGAGGAA; *TBX3* (T-box transcription factor 3) F: GTCGGGAAGGCGAATG TTTC, R: ACGACAGTCATCAGCAGCTA; *TCF7L2*: F: CCTGGCACCGT AGGACAAATC R: GAGGGAACCTGGACATGGAAGC; *TDO2* (tryptophan 2,3-dioxygenase) F: GAGGAACAGGTGGCTGAATTT R:GC TCCCTGAAGTGCTCTGTA. All results were normalized to the mRNA abundance of the housekeeping gene *peptidyl-prolyl cis-trans isomerase E (PPIE)*.

Determination of the Relative Abundance of Mitochondrial DNA

The abundance of mitochondrial DNA (mtDNA) was quantified as described previously [12].

Western Blot Analysis. Western blotting analyses were performed as described previously [12], using the following primary antibodies (Target, Manufacturer, Reference, Dilution factor): ATP synthase α, Life Technologies, A21350, 1:1,000; ATP synthase β, Life Technologies, A21351, 1:2,000; COX I (Cytochrome c oxidase, subunit 1), Abcam, Cambridge, UK, http://www.abcam.com, ab14705, 1:2000; COX II (Cytochrome c oxidase, subunit 2), Abcam, ab110258, 1:2000; COX IV (Cytochrome c oxidase, subunit 3), Life Technologies, A21348, 1:500; Histone 3, Cell Signaling Technology, Danvers, MA, https://www.cellsignal.com, #4499, 1:5,000; PGC-1α (peroxisome proliferator-activated receptor gamma, coactivator 1 alpha), Santa Cruz Biotechnology, Dallas, TX, https://www.scbt.com, SC-13067, 1:500; TCF7L2, Cell Signaling Technology, #2569, 1:1,000; ubiquinol-cytochrome c reductase, complex III subunit VII (UQCRQ), Proteintech, 14975–1-AP, 1:2,000.

Respiration Assays

The extracellular flux analyzer XF96 and the XF Cell Mito Stress Test Kit (Seahorse Biosience, North Billerica, MA) were used to perform metabolic profiling and assess mitochondrial function [13]. The day before the assay, equal number of cells was seeded in wells of a XF cell culture plate. A XF cell mito stress test (Seahorse Bioscience, part of Agilent, North Billerica, MA) was performed according to the manufacturer's instructions and using the following chemical concentrations: 1 μM oligomycin, 0.5 μM carbonyl cyanide 4-(trifluoromethoxy) phenylhydrazone (FCCP), 1 μM antimycin A, and 1 μM rotenone. Once oxygen consumption rate (OCR) and extracellular acidification rate (ECAR) measurements were performed, cells were lysed in 0.5 N NaOH, and OCR and ECAR measurements were normalized to the protein content of the well. Basal respiration was calculated by substracting the non-mitochondrial oxygen consumption [OCR following the addition of both antimycin A and rotenone (mitochondrial complex III and I inhibitors, respectively)] to the basal OCR. ATP coupling efficiency was calculated by substracting the non-mitochondrial oxygen consumption from the OCR following oligomycin addition (an ATP synthase inhibitor) and is expressed as a percentage of the basal respiration. Spare respiratory capacity was calculated by substracting the non-mitochondrial oxygen consumption from the OCR following FCCP (an uncoupling protonophore) addition and is expressed

as a percentage of the basal respiration. For each condition and each donor, 4–12 technical replicates were performed.

Immunofluorescence and Quantification of the Mitochondrial Content per Cell

Cells were seeded on coverslips, fixed with 4% paraformaldehyde for 20 minutes, permeabilized for 5 minutes with phosphate-buffered saline (PBS)-1% Triton X-100, and then incubated for 2 hours with an anti-TOM20 antibody (Santa Cruz Biotechnology, SC-11415, 1:200) (for mitochondria staining) and an anti-β-catenin antibody (BD Transduction Laboratories, part of BD Bioscience, San Jose, CA, http://www.bdbiosciences.com, BD610153, 1:100) (for cytoplasm staining) diluted in PBS-1% bovine serum albumin (BSA). Cells were then incubated for 1 hour with Alexa-labeled secondary antibodies (Molecular Probes, Eugene, OR, now part of Thermo Fischer, https://www.thermofisher.com/us/en/home/brands/molecular-probes/key-molecular-probes-products.html) (1:1,000) and observed by confocal microscopy (Leica Microsystems, Buffalo Grove, IL, Dako (now Agilent Technologies, Santa Clara, CA, http://www.agilent.com/)). The area occupied by the mitochondrial staining per cell was calculated using the ImageJ software.

Immunohistochemistry

Five micrometer thick human liver sections at different stages were deparaffinized and rehydrated in graded alcohol series. Endogenous peroxidase activity was blocked by incubation for 30 minutes in a 1% hydrogen peroxide methanol solution. Antigen retrieval was performed by incubating the sections in citric acid monohydrate solution (pH 9.0) at 98°C for 35 minutes. Non-specific immunostaining was prevented by 1 hour incubation in PBS buffer containing either 5% (immunochemistry) or 10% (immunofluorescence) BSA at room temperature. Slices were incubated for 1 hour with polyclonal antihuman TCF7L2 (Abcam; 1:500), in 0.5% BSA at 37°C. After washing with PBS-Tween-20 0.5% solution, immunostaining detection was visualized by Envision Dako anti-rabbit (Dako), using diaminobenzidine (Sigma) as chromogenic substrate. The nuclei were counterstained using Mayer's hematoxylin for 10 minutes and mounted using Neo-Entellan (Merck, Darmstadt, Germany, http://www.merck.com) for microscopy analysis. The same protocol was used for immunofluorescence staining with anti-TCF7L2 (Abcam; 1:500) and anti-TOM20 (Santa Cruz Biotechnology, SC-11415, 1:200) except that these primary antibodies were revealed by a 1 -hour incubation with the corresponding Alexa-labeled secondary antibodies (Molecular Probes) (1:1,000) before staining nuclei for 5 minutes with 4′,6-diamidino-2-phenylindole. Slides were mounted in fluoromount medium (Sigma).

Statistical Analyses

Depending on the data to compare, two-tailed paired *t* tests (Figs. 1D, 5G–5J) or two-way paired analysis of variance tests (Figs. 1A, 1B, 1C, 3, 4, 5C) were performed, assuming normal distribution of data. In Figure 5G, data were log(2) transformed to ensure homogeneity of variance. To identify the significantly different groups, pairwise multiple comparisons using the Student–Newman–Keuls method were performed (* or #, $p < .05$; ** or ##, $p < .01$; *** or ###, $p < .001$) (when used on a same chart: *, comparisons of Diff vs. day 0; #, comparisons between Diff and Undiff at a particular time point). All statistical analyses were carried out using the SigmaPlot 12.5 software (Systat Software, San Jose, CA, https://systatsoftware.com).

Results

The Mitochondrial Biogenesis and Metabolic Shift Toward OXPHOS Overlap the Decreased Expression of Genes Involved in Pluripotency Pathways During the Commitment of BM-MSCs to the Hepatocytic Lineage

We previously demonstrated a strong mitochondrial biogenesis, characterized by an increase in the abundance of mitochondria, mtDNA and several OXPHOS subunits, in a model of hepatocytic differentiation of human BM-MSCs [12]. To get a deeper insight into the mechanisms regulating this mitochondrial biogenesis, we monitored these parameters over time. We evaluated the abundance of mtDNA, of several OXPHOS subunits (the UQCRQ), the subunits I, II, and IV of the cytochrome C oxidase (COX I, COX II, and COX IV) and the subunits α and β of the ATP synthase and the respiration rate throughout the hepatocytic induction step (from day 0 to day 12 of the differentiation process, lasting 22 days in total) (Fig. 1). A slight but significant induction of mtDNA was detected since the 5th day of differentiation (Fig. 1A). Similarly, several OXPHOS subunits were significantly more abundant after 5 days of differentiation (Fig. 1B, 1C). This resulted, at the functional level, in a significantly increased basal respiration, coupling efficiency (fraction of the basal respiration that is used for ATP production) and spare respiratory capacity (cell's ability to increase substrates and electron flux across the OXPHOS chain to respond to an increased energy demand) of the OXPHOS system, as soon as 5 days of differentiation (Fig. 1D). In addition, the basal ECAR, an undirect measurement of glycolysis, was lower in differentiated BM-MSCs (Fig. 1D). These data support that the mitochondrial biogenesis and metabolic shift toward OXPHOS occurred within the first 5 days of hepatocytic differentiation.

To unveil the mechanisms regulating mitochondrial biogenesis during the differentiation of BM-MSCs into hepatocyte-like cells, we performed transcriptomics analyses at early time points of the differentiation process. Strikingly, analysis of the 10 most enriched pathways among genes upregulated after 5 days of differentiation revealed an enrichment of the "OXPHOS pathway" (Fig. 1E, right panel). Indeed, 30 of 104 (29%) of the OXPHOS subunits referenced in this pathway were upregulated after 5 days of differentiation. These data support the notion that the observed increased OXPHOS activity (Fig. 1D) is at least partly explained by a broad induction of OXPHOS-related genes at the transcript level. We also observed an induction of the "Mitochondrial dysfunction pathway," a pathway that includes mitochondrial proteins frequently mutated or dysregulated in mitochondrial diseases, including OXPHOS subunits, metabolic enzymes (e.g., TCA cycle) and ROS detoxifying enzymes. This observation supports the notion that many mitochondrial genes—besides OXPHOS—are upregulated during differentiation. The upregulation of ROS detoxifying enzymes has also been reported during the osteogenic differentiation of MSC and would protect the differentiating cells from the increased generation of ROS accompanying the switch toward OXPHOS metabolism [14]. In agreement with the progressive acquisition of a hepatic fate, an induction of metabolic pathways related to cholesterol synthesis, a typical hepatic function, was also observed. On the other hand, pathways involved in the regulation of stemness and pluripotency, including the "human ESC pluripotency," "Wnt/β-catenin signaling," and "transforming growth factor

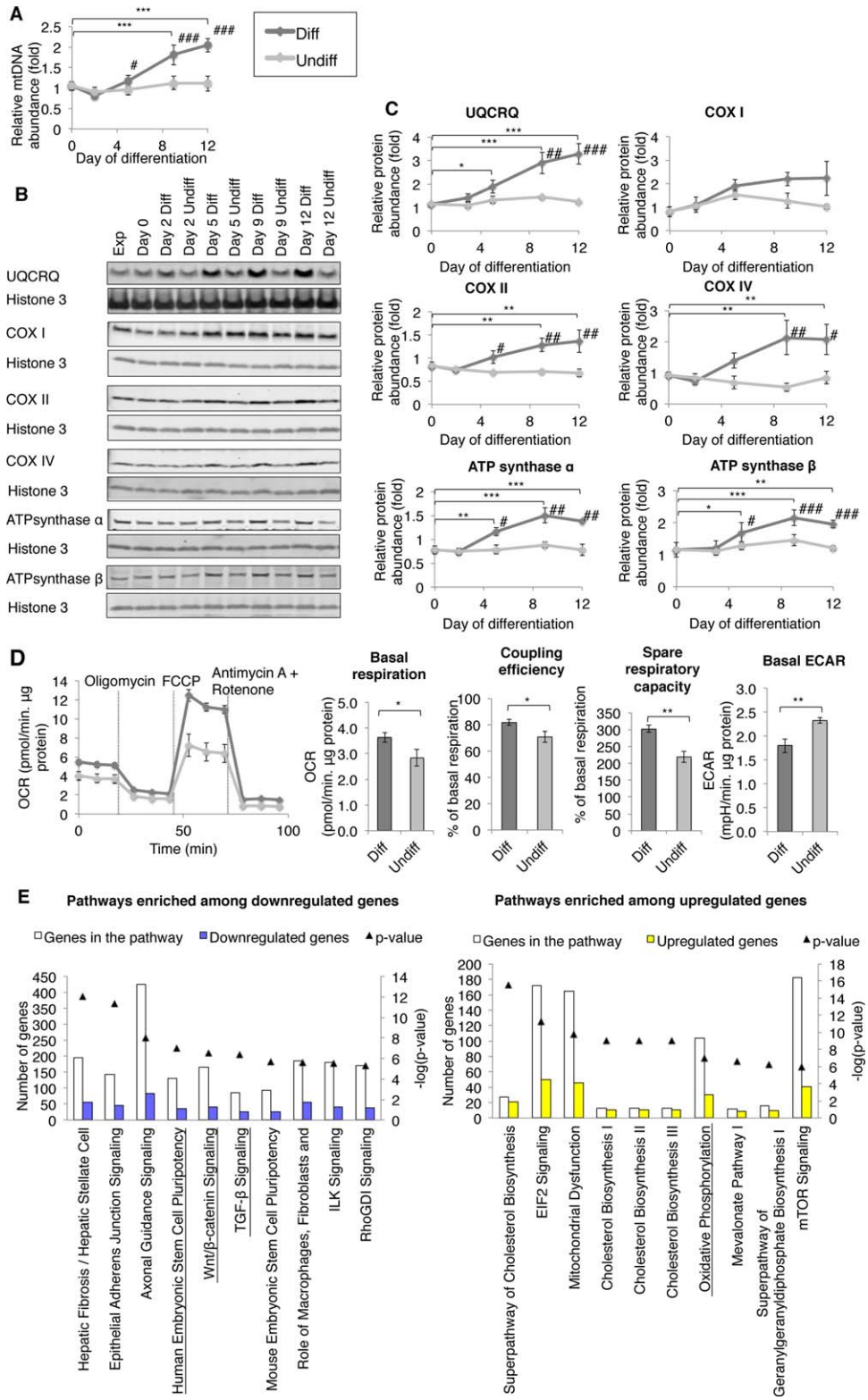

Figure 1. Mitochondrial biogenesis and metabolic shift toward oxidative phosphorylation (OXPHOS) occur early during the hepatocytic differentiation. **(A)**: Mitochondrial DNA abundance. **(B)**: Abundance of several OXPHOS subunits analyzed by Western blot. **(C)**: Quantification of the signal intensity. **(D)**: Metabolic profiling and assessment of the mitochondrial function of differentiated and undifferentiated cells at day 5. **(E)**: Top 10 enriched pathways among upregulated and downregulated genes after 5 days of differentiation, ranked according to increasing *p* values of the enrichment. (A, C): Data are presented as the mean ± SEM, relative to cells in expansion. (D): Data are presented as the mean ± SEM. (A–C) $n = 3$, (D) $n = 4$ independent experiments. * or #, $p < .05$; ** or ##, $p < .01$; *** or ###, $p < .001$; *, comparisons versus day 0; #, comparisons between Diff and Undiff. Abbreviations: ECAR, extracellular acidification rate; EIF2, eukaryotic translation initiation factor 2; FCCP, carbonyl cyanide 4-(trifluoromethoxy)phenylhydrazone; ILK, integrin linked kinase; mTOR, mammalian target of rapamycin; OCR, oxygen consumption rate; TGF, transforming growth factor.

beta (TGF-β) signaling" pathways, were strongly enriched among the genes downregulated after 5 days of differentiation (Fig. 1E, left panel). Thus, the induction of mitochondrial biogenesis overlaps the downregulation of genes belonging to pathways involved in the control of stem cell pluripotency, during the early hepatocytic differentiation of BM-MSCs. Supporting the loss of the mesenchymal phenotype and promotion of the hepatic differentiation, a downregulation of genes involved in the "hepatic fibrosis pathway "(that includes the TGF-β pathway - an inhibitor of hepatocyte proliferation and differentiation [15]- and downstream of it, expression of collagens) was observed. Similarly, due to the important change in morphology (cell elongation) observed during the first step of the differentiation process, the "epithelial adherens junction pathway" (involving members of the TGF-β pathway, catenins, tubulins, and actins) was also statistically downregulated.

Identification of Predicted Co-Regulators of Mitochondrial Biogenesis and Stem Cell Commitment to Differentiation

A lack of understanding currently resides in the mechanisms connecting, on the one hand, the increase in mitochondrial biogenesis and function and, on the other hand, the loss of pluripotency and differentiation of stem cells. We hypothesized that these two concomitant processes might be controlled by common regulators. We thus investigated the putative upstream regulators of DEGs (Supporting Information Table S1) related to the mitochondria (Supporting Information Table S2) and to stem cell pluripotency or differentiation (Supporting Information Table S3), seeking to identify putative common regulators of the two processes (Supporting Information Table S4, S5, respectively) (the strategy developed to identify those common regulators is detailed in the Material and Method section and illustrated in Fig. 2).

Using IPA, 40 predicted co-regulators were identified, of which 9 displayed after 3 and/or 5 days of differentiation a differential expression consistent with their predicted activation status (Table 1). Among them, *HIF-1α* is the candidate predicted to be the most strongly repressed during differentiation, while *PGC-1α*, predicted to be activated during differentiation, is the candidate displaying the highest differential expression after 5 days of differentiation (Table 1). Noteworthy, the efficiency of our bioinformatics approach in identifying co-regulators of mitochondrial biogenesis and cell commitment to differentiation is supported by the identification of *HIF-1α* as one of those putative co-regulators. Indeed, in ESCs, HIF-1α positively regulates pluripotency while inhibiting mitochondrial biogenesis and function, through its binding to the promoter of pluripotency genes and *PGC-1α*, resulting in transcriptional activation and inhibition, respectively [4]. Since HIF-1α is not expressed at the protein level in adult BM-MSCs (unpublished personal data and [16]), we decided to further focus on *PGC-1α*. Importantly, PGC-1α is reported to interact with multiple transcriptional regulators also identified as putative co-regulators of mitochondrial biogenesis and stem cell differentiation, including PPAR-α [17], PPAR-γ [18], the hepatocyte nuclear factor-4α (HNF-4α), and the glucocorticoid receptor (GR or NR3C1) [19] (Table 1). These observations suggest that PGC-1α might exert a broad effect on the co-regulation of mitochondrial biogenesis and cell differentiation. We thus investigated whether *PGC-1α* induction was required for the hepatocytic differentiation of BM-MSCs and the associated mitochondrial biogenesis.

Repressing PGC-1α Induction Partly Prevents Mitochondrial Biogenesis and Hampers BM-MSC Hepatocytic Differentiation

PGC-1α mRNA is strongly induced during hepatocytic differentiation (Fig. 3A), resulting in a modest but significant increase in the protein level (day 5 Diff vs. day 0: $p = .032$; day 12 Diff vs. day 0: $p = .002$; day 22 Diff vs. day 0: $p = .003$) (Fig. 3D, 3E). To test whether the ∼1.5-fold increase in PGC-1α abundance was responsible for the increased mitochondrial biogenesis and function, we used shRNA against *PGC-1α*. We repressed the induction of *PGC-1α* mRNA by 54%, 52% and 64% after 5, 12 and 22 days of differentiation, respectively (Fig. 3A). At the protein level, we inhibited by 93%, 53% and 49% the differentiation-induced increases in PGC-1α expression observed at these respective time points (Fig. 3E). The fact that we only partially repressed PGC-1α induction, without repressing its abundance to lower levels than what is observed in expanding stem cells (i.e., not lower than the fold change treshold set to 1), allowed us to assess the requirement of PGC-1α induction, specifically (rather than basal expression), for the mitochondrial biogenesis and commitment to the hepatocytic lineage.

The repression of PGC-1α led to a modest repression of mtDNA relative abundance, mainly in undifferentiated cells and cells differentiated for 5 days (Fig. 3B). To determine whether other regulators were involved in the regulation of mtDNA abundance, we analyzed the mRNA abundance of several major regulators of mtDNA replication, including *POLG*, which encodes the catalytic core of the DNA polymerase γ involved in mtDNA replication; *TFAM*, a mitochondrial transcription factor whose expression has been correlated with mtDNA abundance [20] and of the *mitochondrial RNA polymerase POLRMT*, which is involved in mtDNA replication by synthetizing an RNA primer required for the initiation of mtDNA replication [21]. Modest changes were observed in the expression of those regulators during differentiation (Supporting Information Fig. S1). Moreover these changes were not consistent with the mtDNA induction profile observed during differentiation. More interestingly, we found that the mRNA encoding the DNA polymerase γ accessory subunit *POLG2*, was increased 1.5- to twofolds during the hepatocytic differentiation. Incidentally, we found that the repression of PGC-1α led to a modest but significant repression of *POLG2* induction (Fig. 3B). Altogether, these data suggest that PGC-1α regulates *POLG2* expression, regulating itself mtDNA replication. However, the partial inhibition of PGC-1α induction - and hence, of *POLG2* induction, only leads to minor differences in mtDNA abundance.

In contrast, the repression of PGC-1α drastically prevented the increase in mitochondrial content per cell observed by the end of the hepatocytic induction step (Fig. 3C). The strong impact of PGC-1α on mitochondrial abundance might be related to its ability to co-activate several families of nuclear transcription factors involved in mitochondrial biogenesis [5]. Similarly, PGC-1α repression was associated with a significant decrease in the protein abundance of the subunits α and β of the ATP synthase and of the subunit UQCRQ of the complex III (Fig. 3D, 3E). Altogether, the partial repression of PGC-1α

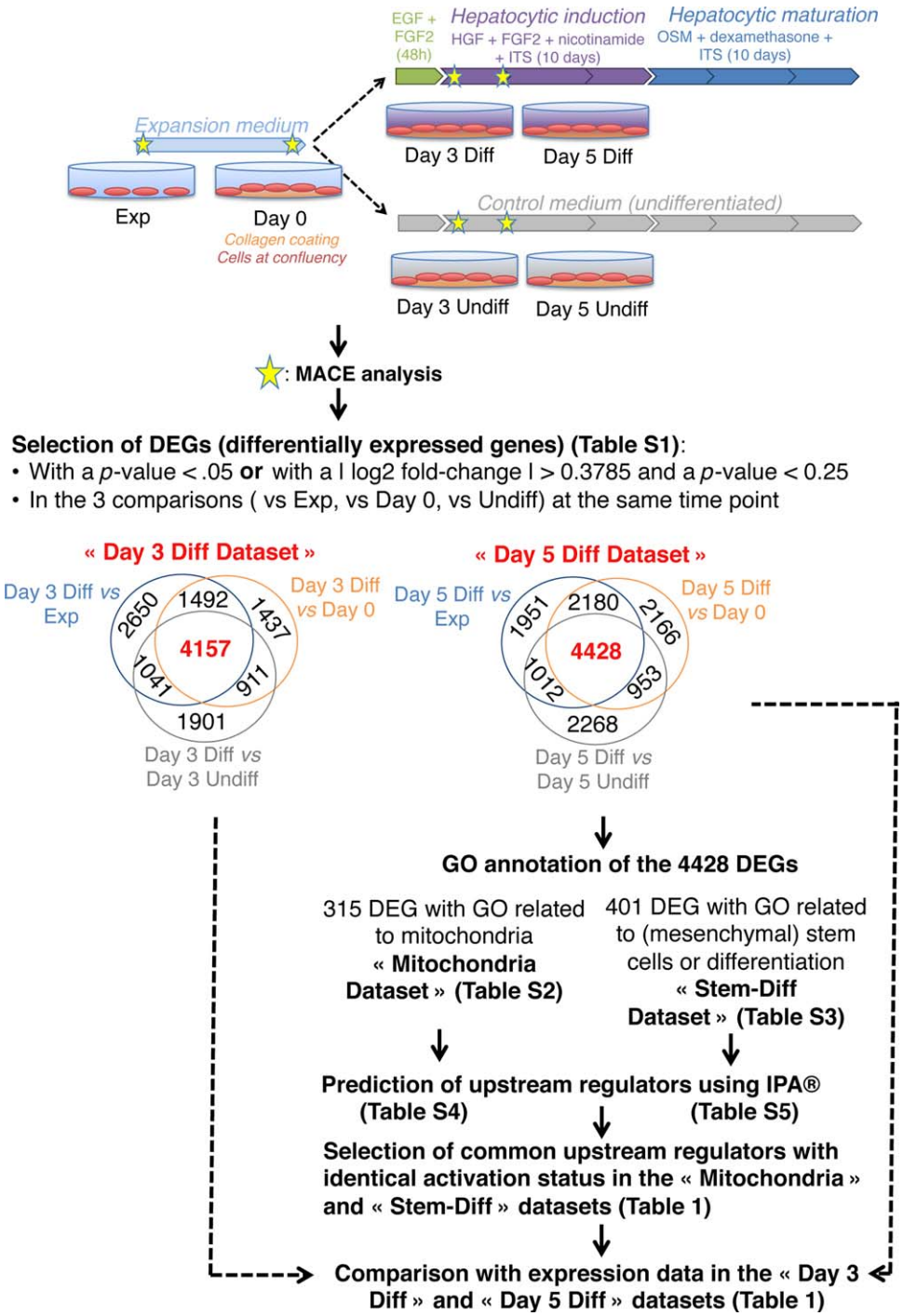

Figure 2. Strategy developed to identify common transcriptional regulators of gene expression changes related to stem cell differentiation and mitochondria. Transcriptomics analyses were performed at early time-points of the differentiation process and differentially expressed genes (DEGs) were identified (see Material and Method section for further details). Gene ontology (GO) terms were retrieved for DEGs at day 5 of differentiation. DEGs were then sorted based on their GO annotations: one set was established with genes containing annotations related to mitochondria ("Mitochondria dataset"), another one with genes containing annotations related to (mesenchymal) stem cells or differentiation ("Stem-diff dataset"). The "upstream analysis" function of IPA was used to identify the putative regulators of these two lists of DEGs. This function, which relies on a database containing the expected effects between transcriptional regulators and their target genes, retrieves the transcriptional regulators that are putatively involved in the differential expression of a list of genes. It also predicts whether these regulators are likely activated or inhibited, based on the expression value of their targets. The common regulators of the Stem-diff dataset and mitochondria dataset were subsequently selected, and their expression profile at day 3 and/or 5 of differentiation was retrieved (see Table 1). Abbreviations: DEG, differentially expressed gene; EGF, epidermal growth factor; FGF, fibroblast growth factor; GO, gene ontology; HGF, hepatocyte growth factor; ITS, insulin–transferrin–selenium; MACE, massive analysis of cDNA ends; OSM, oncostatin M.

Table 1. Identification of common predicted regulators of the differentially expressed genes with GO related to mitochondria and stem cell differentiation and comparison of their predicted activation status and actual expression at the mRNA level

		Predicted activation status of the TR based on gene expression of the mitochondria dataset			Predicted activation status of the TR based on gene expression of the Stem-diff dataset			Differential expression of the TR after 3 days of differentiation			Differential expression of the TR after 5 days of differentiation		
	Transcriptional regulator (TR)	Activation *z*-score	*p* value of overlap	Targets	Activation *z* score	*p* value of overlap	Targets	Day 3 dataset	Log2FC (day 3 diff vs. exp)	*p* value (day 3 diff vs. exp)	Day 5 dataset	Log2FC (day 5 diff vs. exp)	*p* value (day 5 diff vs. exp)
Differential expression consistent with the predicted activation status	PGC-1α	2.21	1.25E-13	19	1.43	2.39E-04	10	/	1.15	2.22E-01	Upregulated	3.25	4.36E-08
	PPAR-γ	2.60	4.93E-07	19	1.41	6.92E-21	40	Upregulated	1.68	1.26E-15	Upregulated	1.79	6.69E-22
	SREBF1	1.12	2.29E-03	8	1.57	1.74E-06	14	/	1.22	1.96E-38	Upregulated	1.66	1.38E-98
	IFI16	1.66	1.02E-04	6	1.28	4.88E-06	8	Upregulated	0.47	1.97E-14	Upregulated	0.97	2.17E-81
	STAT6	1.46	3.94E-02	6	1.13	1.47E-07	16	Upregulated	0.50	8.79E-13	Upregulated	0.38	3.45E-09
	NUPR1	−1.47	3.18E-02	12	−1.07	3.15E-04	20	Downregulated	−1.01	2.73E-179	Downregulated	−0.46	1.78E-56
	HIF-1α	−1.43	1.56E-08	19	−2.39	1.54E-26	42	Downregulated	−1.01	4.80E-175	Downregulated	−1.05	7.88E-230
	EGR2	−0.34	7.03E-03	6	−0.62	5.29E-10	16	Downregulated	−0.98	2.44E-05	Downregulated	−2.11	9.59E-17
	STAT4	−0.66	2.26E-02	7	−0.59	6.86E-05	13	Downregulated	−2.09	1.63E-11	Downregulated	−2.19	1.45E-14
Expression change consistent with the predicted activation status but not statistically significant in all comparisons	MYCN	1.32	1.24E-03	10	0.93	4.28E-09	20	/	0.83	7.68E-01	/	1.12	6.45E-01
	PPAR-α	2.07	2.11E-11	26	1.85	1.92E-08	25	/	0.68	1.58E-04	/	0.26	1.29E-01
	HNF4-α	3.13	2.24E-10	61	1.70	3.27E-02	44	/	0.83	7.68E-01	/	0.12	9.68E-01
	VHL	1.89	3.75E-06	10	1.70	1.45E-09	15	/	0.25	8.39E-02	/	0.07	5.97E-01
	SIRT1	−0.24	3.60E-04	7	−0.98	1.01E-06	11	/	−0.12	5.33E-01	/	−0.19	2.63E-01
	MYC	−0.37	1.17E-14	43	−0.24	1.34E-22	47	/	0.15	8.29E-02	/	−0.35	3.53E-05
	ESR2	−1.20	1.62E-02	7	−2.21	3.26E-12	22	/	−0.17	9.44E-01	/	−0.88	7.16E-01
Undetected mRNA	C/EBP-α	0.99	2.30E-02	10	1.31	1.35E-10	18	/	NA	NA	/	NA	NA
	GATA1	2.00	1.65E-02	6	0.64	9.99E-11	19	/	NA	NA	/	NA	NA
	GATA3	1.97	3.93E-02	4	0.27	2.73E-07	11	/	NA	NA	/	NA	NA
	GATA4	1.18	2.90E-02	4	0.08	5.66E-06	10	/	NA	NA	/	NA	NA
	NR1H4	−1.89	5.76E-02	4	−1.18	2.61E-06	11	/	NA	NA	/	NA	NA
	PDX1	−0.38	4.56E-04	9	−0.58	2.77E-14	32	/	NA	NA	/	NA	NA
Expression change not consistent with the predicted activation status	ESR1	−0.11	2.62E-02	10	−0.82	5.89E-19	38	/	0.37	5.68E-01	/	1.12	3.07E-02
	PGC-1β	−1.11	3.36E-03	4	−0.57	1.14E-03	5	/	0.10	9.25E-01	/	0.38	6.63E-01
	HTT	−1.45	1.07E-09	32	−0.40	3.21E-15	46	Upregulated	0.33	2.66E-02	Upregulated	0.28	4.10E-02
	TP53	0.97	4.76E-15	54	0.34	1.13E-34	47	Downregulated	−1.10	3.53E-21	/	−0.12	1.79E-01
	FOXO3	2.24	1.02E-05	10	0.02	5.39E-08	14	Downregulated	−0.78	8.17E-09	/	−0.17	1.11E-01
	HSF1	0.31	7.36E-06	11	1.41	4.34E-07	14	/	−0.29	7.48E-02	/	−0.23	1.15E-01
	MEF2C	1.20	1.77E-03	5	0.39	8.56E-04	6	/	−0.25	3.76E-01	/	−0.28	2.62E-01
	EPAS1	1.97	1.38E-02	6	0.54	5.67E-17	24	Downregulated	−1.49	9.93E-226	/	−0.40	7.48E-31
	NFE2L2	2.43	4.28E-04	14	0.25	9.47E-08	24	Downregulated	−0.47	1.31E-11	Downregulated	−0.41	2.32E-11
	ETS2	1.22	6.72E-03	4	0.23	4.88E-06	8	Downregulated	−0.86	1.49E-02	/	−0.46	1.24E-01
	NR3C1	0.32	6.51E-04	19	1.16	4.18E-17	46	Downregulated	−0.30	1.04E-06	Downregulated	−0.65	2.92E-28
	REL	1.22	1.75E-02	5	1.64	6.81E-08	13	/	0.05	9.34E-01	/	−0.66	3.27E-01
	RB1	1.15	1.93E-02	8	0.48	2.88E-14	27	/	−0.30	1.81E-02	Downregulated	−0.79	1.02E-10
	MUC1	2.22	2.93E-05	5	0.94	1.41E-08	8	Downregulated	−1.90	8.21E-11	Downregulated	−0.84	1.42E-04
	FOXA1	0.30	1.27E-02	5	2.13	2.73E-09	14	/	0.83	6.77E-01	/	−0.88	7.16E-01
	WT1	0.15	3.42E-02	5	0.89	1.59E-13	20	/	0.83	6.77E-01	/	−0.88	7.16E-01
	GFI1	1.00	2.69E-02	4	1.80	2.22E-08	12		−1.75	3.32E-01		−1.47	3.44E-01
	NR4A3	1.11	5.41E-05	6	2.38	2.24E-05	7	/	−4.38	6.63E-08	/	−2.77	5.45E-07

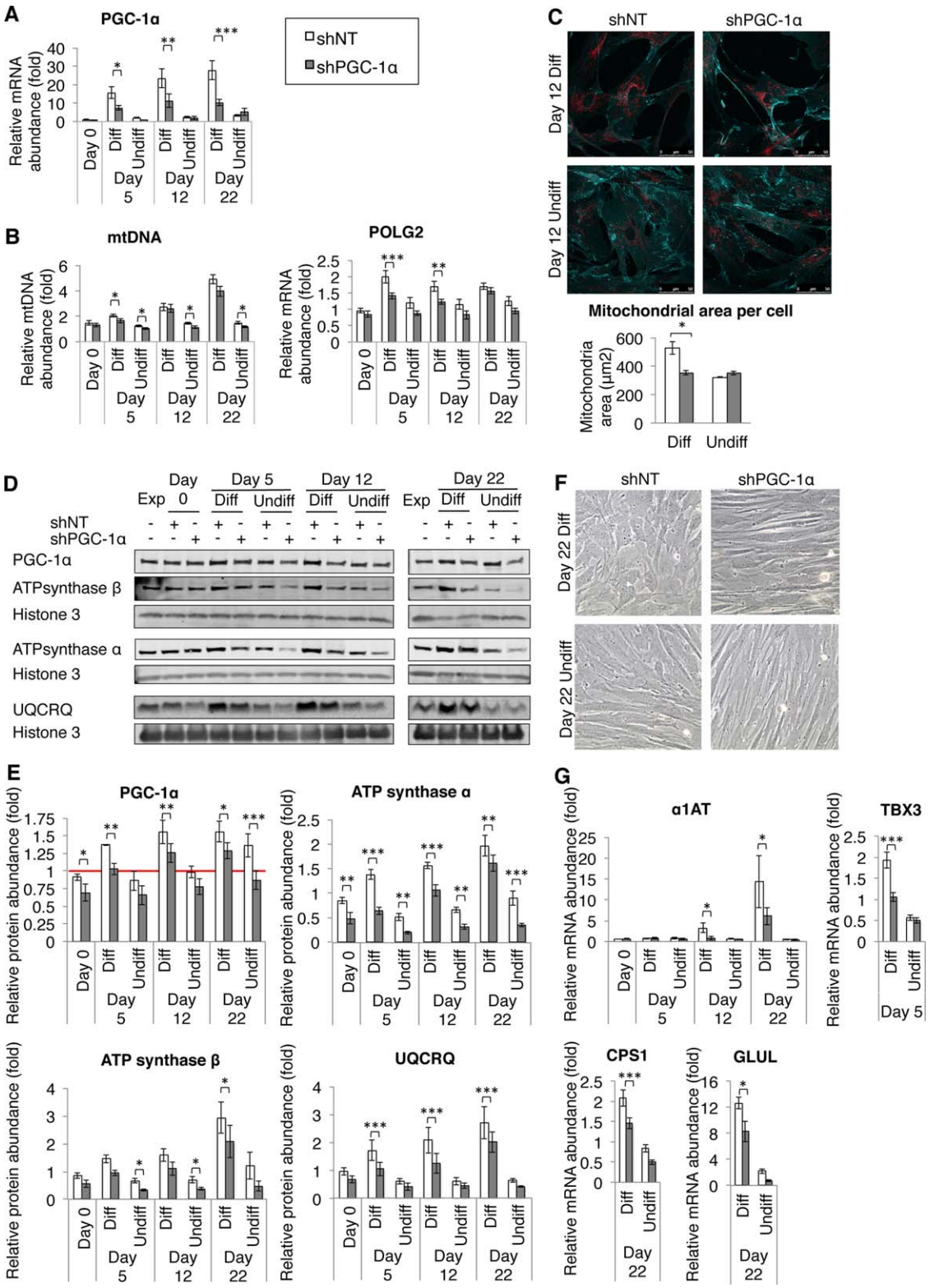

Figure 3. Repressing peroxisome proliferator-activated receptor gamma coactivator-1 alpha (PGC-1α) induction prevents mitochondrial biogenesis and hampers hepatocytic differentiation. Cells were transduced with non-target control shRNA (shNT, white bars) or specific shRNA against PGC-1α (shPGC-1α, grey bars) and submitted to hepatocytic differentiation. **(A)**: PGC-1α mRNA abundance. **(B)**: Mitochondrial DNA abundance and DNA polymerase gamma-2 mRNA abundance. **(C)**: Immunofluorescence of the mitochondrial network, visualized by a TOM20 immunostaining (red). Cells are counterstained using a β-catenin immunostaining (cyan blue). The mitochondrial content per cell was determined by calculating the area, per cell, occupied by the mitochondrial network. Ten cells were analyzed per condition and per experiment, $n = 3$ independent experiments. Scale bar = 50 µm. **(D)**: Abundance of several oxidative phosphorylation subunits analyzed by Western blot. **(E)**: Quantification of the Western blot signal intensity. **(F)**: Morphology of cells at the end of the differentiation process (day 22), observed by phase-contrast microscopy. Scale bar = 250 µm. **(G)**: mRNA abundance of differentiation markers. (A, B, E, G): Data are presented as the mean ± SEM, relative to untransduced cells in expansion. (C): Data are presented as the mean ± SEM. (A, B, D, E, F, G): $n = 5$ independent experiments. For clearness, only significant differences between transduction conditions (shNT vs. shPGC-1α) were illustrated (*, $p < .05$; **, $p < .01$; ***, $p < .001$). Abbreviations: CPS1, carbamoyl phosphate synthetase 1; GLUL, glutamine synthetase; PGC-1α, peroxisome proliferator-activated receptor gamma coactivator-1 alpha; shNT, non-target control shRNA; shPGC-1α, shRNA against PGC-1α; UQCRQ, ubiquinol-cytochrome c reductase, complex III subunit VII.

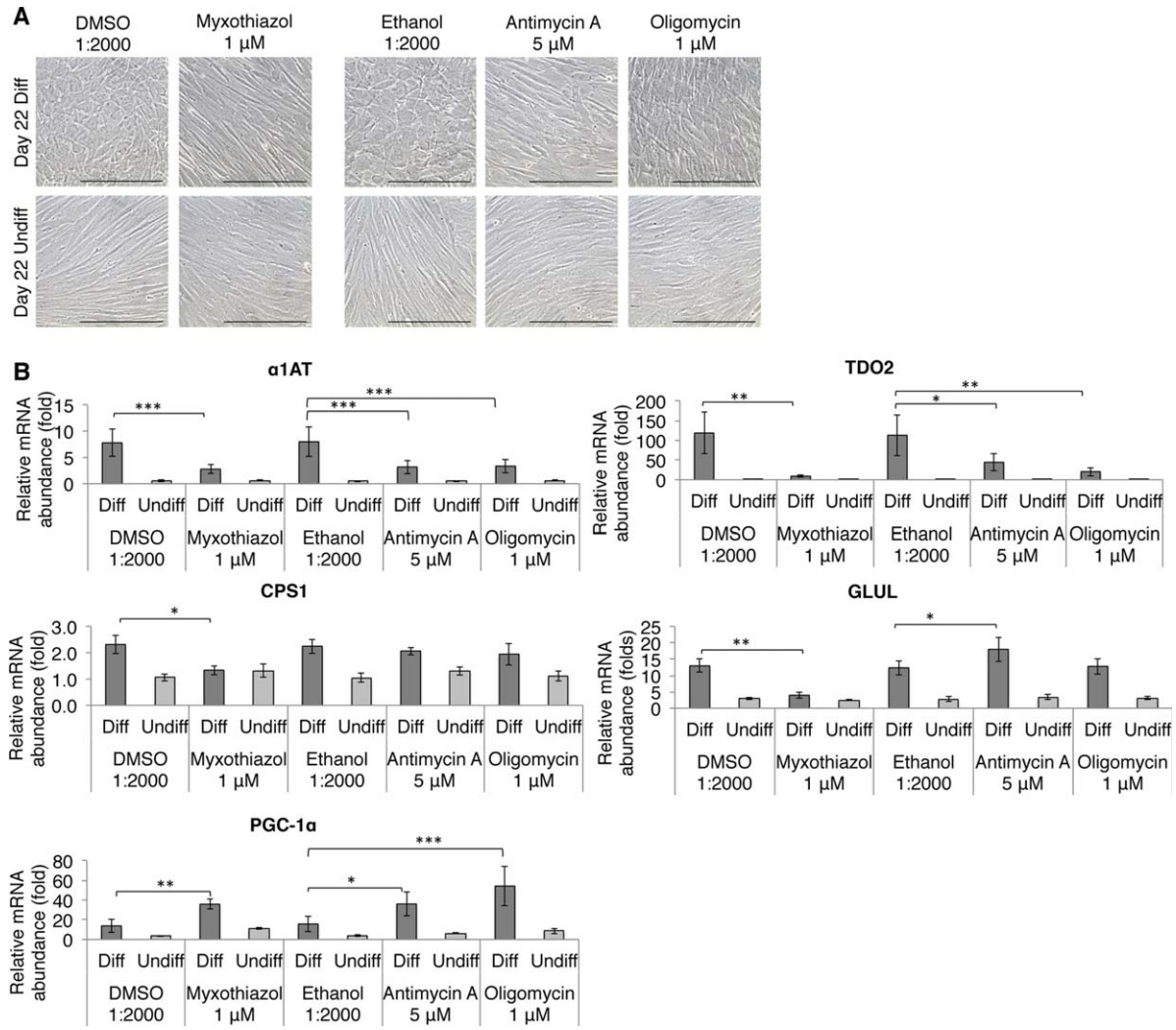

Figure 4. Inhibiting oxidative phosphorylation hampers hepatocytic differentiation. **(A)**: Morphology of cells at the end of the differentiation process (day 22), observed by phase-contrast microscopy. Scale bar = 250 μm. **(B)**: mRNA abundance of differentiation markers and peroxisome proliferator-activated receptor gamma coactivator-1 alpha. Data are presented as mean ± SEM (n = 4 independent experiments) relative to untreated cells in expansion. For clearness, only significant differences between molecules and their vehicle were illustrated (*, $p < .05$; **, $p < .01$; ***, $p < .001$). Abbreviations: CPS1, carbamoyl phosphate synthetase 1; DMSO, dimethyl sulfoxide; GLUL, glutamine synthetase; PGC-1α, peroxisome proliferator-activated receptor gamma coactivator-1 alpha.

induction partly impaired the mitochondrial biogenesis observed during the hepatocytic differentiation of BM-MSCs.

We next asked whether limiting the induction of PGC-1α would also disturb the hepatocytic differentiation or not. Strikingly, the acquisition of the typical hepatocyte-like polygonal shape, normally observed by the end of the differentiation process, was strongly hampered in cells transduced with shRNA against PGC-1α (Fig. 3F). At the mRNA level, the induction of *TBX3*, a transcription factor expressed in hepatoblasts [22] and induced during the early commitment to hepatocytic differentiation, was completely abrogated in shRNA against PGC-1α (shPGC-1α)-transduced cells (Fig. 3G). Moreover, a delayed and reduced induction of the hepatocytic marker α-1-antitrypsin (*α1AT*) was observed in shPGC-1α-transduced cells. Similarly, a reduced induction of the hepatic/periportal gene *CPS1* and of the pericentral marker glutamine synthase (*GLUL*) was observed by the end of the differentiation process (Fig. 3G). Altogether, these results support that PGC-1α is required for the mitochondrial biogenesis, for the morphological maturation into hepatocyte-like cells and for the acquisition of hepatic gene expression of both periportal and perivenous regions.

OXPHOS Activity Is Required for the Differentiation into Hepatocyte-like Cells

PGC-1α co-activates several transcription factors involved in liver development and hepatic gene expression, including CCAAT/enhancer binding protein β [23], HNF-4α [19], the forkhead box protein O1 [24], and the glucocorticoid receptor [25]. Therefore, PGC-1α might contribute to hepatocytic differentiation directly, by transactivating hepatic transcription factors, and/or undirectly, by inducing mitochondrial biogenesis and function. To test the latter possibility, we differentiated BM-MSCs in the presence of inhibitors of the mitochondrial complex III (myxothiazol and antimycin A) and V (oligomycin). Inhibiting OXPHOS activity prevented the acquisition of the

hepatocyte-like polygonal shape (Fig. 4A). Importantly, the induction of the hepatocytic markers *α1AT* and *tryptophan 2,3-dioxygenase (TDO2)* is strongly reduced upon OXPHOS inhibition (Fig. 4B). Myxothiazol treatment also inhibited the induction of the periportal gene *CPS1* and of the pericentral marker *GLUL* (Fig. 4B). Importantly, the inhibitors did not induce a strong ATP shortage (Supporting Information Fig. S2) nor enhanced cell apoptosis (M Caruso, unpublished observations), supporting the requirement for mitochondrial activity, specifically, for hepatocytic differentiation. Since the induction of *PGC-1α* mRNA is enhanced in the presence of the different OXPHOS inhibitors (Fig. 4B)—likely as a compensatory mechanism for the decreased OXPHOS activity—these data support that PGC-1α contributes to hepatocytic differentiation at least partly through its ability to induce mitochondrial biogenesis and function. Nonetheless, we did not observe any change in *TBX3* induction in the presence of the OXPHOS inhibitors (unpublished observations), unlike upon PGC-1α repression (Fig. 3G). These observations suggest that PGC-1α might in addition stimulate hepatocytic differentiation independently of OXPHOS.

The TCF7L2-PGC-1α Axis Links Mitochondrial Biogenesis and Metabolic Shift to the Early Commitment to Hepatocytic Differentiation

We next focused deeper on the upstream regulators of the interplay between stem cell differentiation and mitochondrial biogenesis. We hypothesized that the expression of *PGC-1α* itself might be controlled by regulators of stem cell differentiation. Using IPA, we retrieved the transcriptional regulators of *PGC-1α* expression. We selected those that were differentially expressed after 3 or 5 days of differentiation and which expression changes were consistent with the induction of *PGC-1α*, based on litterature data (Fig. 5A; Supporting Information Table S6). *TCF7L2* appeared as a strong candidate as it is a downstream effector of the Wnt/β-catenin signaling pathway [26] predicted to negatively affect *PGC-1α* expression according to IPA. Interestingly, systems biology network analyses revealed that *TCF7L2* is functionally associated with the stemness regulator *SOX2* in human ESCs [27], emphasizing its possible function as a molecular node connecting stem cell loss of pluripotency to the initiation of mitochondrial biogenesis. In addition, the repression of Wnt/β-catenin signaling is required for early liver specification [28]. Accordingly, we observed a strong repression of *TCF7L2* expression, particularly at early time points of the hepatocytic differentiation (Fig. 5B, 5C), as well as a global downregulation of genes involved in the Wnt/β-catenin signaling pathway, after 5 days of differentiation (Fig. 1E). Besides, we evidenced a progressive downregulation of TCF7L2 expression during human liver development (Fig. 5D, 5E). Thus, we hypothesized that the downregulation of the Wnt/β-catenin signaling and of TCF7L2 expression during hepatic differentiation and maturation might trigger PGC-1α induction, mitochondrial biogenesis and metabolic shift. Supporting this hypothesis, we found that in neonatal livers, hepatocytes with a high TCF7L2 staining in the nuclei had a very limited mitochondrial network, while those displaying the largest mitochondrial networks had no detectable expression of TCF7L2 (Fig. 5F).

To test this hypothesis, we repressed *TCF7L2* in expanding BM-MSCs and assessed whether *TCF7L2* repression would be sufficient to induce mitochondrial biogenesis, independently of the stimulation with differentiation cocktails. Using lentiviral-mediated transduction of shRNA against *TCF7L2*, we repressed TCF7L2 mRNA and protein abundance by 56% and 49%, respectively (Fig. 5G–5I). In agreement with our hypothesis, TCF7L2 repression resulted in an increased abundance of PGC-1α transcript (Fig. 5G) and in a 17% increase in PGC-1α protein abundance (Fig. 5H, 5I). Furthermore, the repression of TCF7L2 resulted in a significant increase in the abundance of several OXPHOS subunits, including UQCRQ, COX I, COX II, COX IV, and the subunit β of the ATP synthase (Fig. 5H, 5I) and in an increased basal respiration rate (Fig. 5J). Altogether, TCF7L2 repression increases PGC-1α expression and OXPHOS activity in BM-MSCs.

Discussion

In this study, we postulated that mitochondrial biogenesis and stem cell differentiation might be controlled by common transcriptional regulators. We found that PGC-1α was necessary for the induction of mitochondrial biogenesis and also for the acquisition of hepatic gene expression during hepatic differentiation.

As previously mentioned, PGC-1α co-activates several hepatic transcription factors, such as CCAAT/enhancer binding protein β [23], HNF-4α [19], the forkhead box protein O1 [24], and the glucocorticoid receptor [25], in addition to its ability to co-activate mitochondrial transcriptional regulators such as the estrogen-related receptor α (ERRα) or nuclear respiratory factor-2 [5]. While we evidenced that OXPHOS activity is required for the hepatocytic differentiation of BM-MSCs, further studies are required to investigate the potential mitochondrial-independent role of PGC-1α in that process. PGC-1α has been demonstrated to regulate different loci through its interaction with mitochondrial or hepatic transcription factors [23]. Therefore, it would be interesting to investigate the loci and transcription factors bound by PGC-1α at different time points of the hepatocytic differentiation of BM-MSCs, to further elucidate its involvement in the co-regulation of hepatocytic differentiation and mitochondrial biogenesis. PGC-1α is also reported to regulate chondrogenesis by co-activating the transcription factor SRY-related high mobility group-Box gene 9 (Sox9) in MSCs [30]. These data suggest that PGC-1α may co-regulate mitochondrial biogenesis and stem cell differentiation into several lineages, by co-activating different transcriptional regulators.

Although we restricted our studies to the transcriptional control of PGC-1α, it is worth mentioning that post-translational modifications of PGC-1α affect its activity, including its ability to coactivate different transcription factors. For example, the phosphorylation of PGC-1α downstream of the S6 kinase, activated upon feeding in the liver, reduces the ability of PGC-1α to coactivate HNF-4α, but not ERRα or PPARα [31]. This modification alters the ability of PGC-1α to control the expression of neoglucogenic but not mitochondrial genes [31]. Therefore, post-translational modifications of PGC-1α likely control its ability to regulate mitochondrial biogenesis and stem cell differentiation toward different lineages. This remains a complex area of research, given the high number of post-translational modifications PGC-1α is subjected to [32].

Upstream of PGC-1α, we found that TCF7L2 negatively controls mitochondrial biogenesis and metabolic shift toward

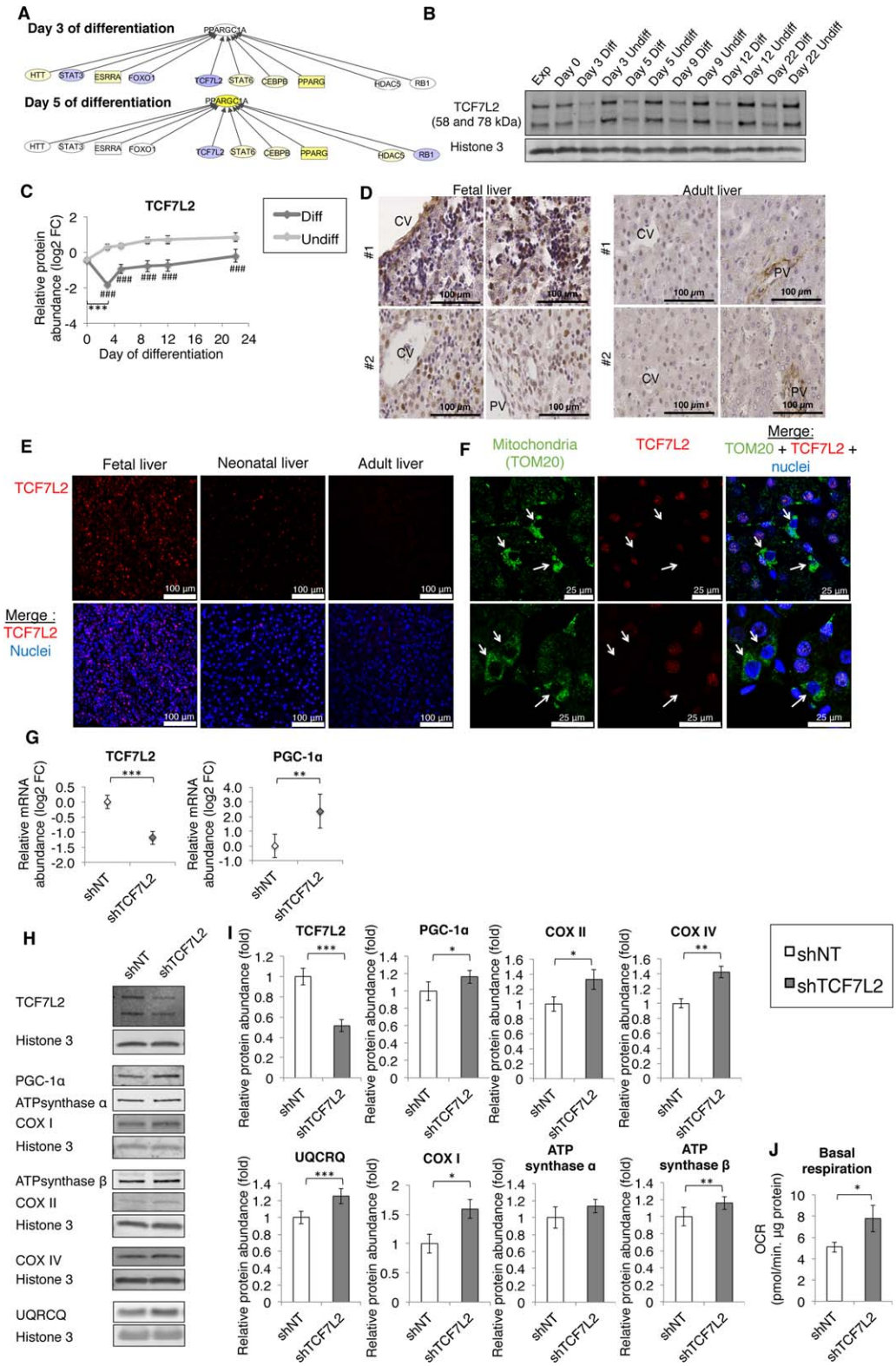

Figure 5. Transcription factor 7-like 2 (TCF7L2) is repressed during hepatocytic differentiation and its repression increases peroxisome proliferator-activated receptor gamma coactivator-1 alpha (PGC-1α) expression, mitochondrial biogenesis, and function. **(A)**: Transcriptional regulators of PGC-1α (PPARGC1A) were retrieved using IPA. The regulators displaying a differential expression at day 3 and/or day 5 of differentiation (purple, downregulated; yellow, upregulated) consistent with the induction of PGC-1α are illustrated. **(B)**: Abundance of TCF7L2 analyzed by Western blot. **(C)**: Quantification of the Western blot signal intensity. Data are expressed relative to expanding cells and presented as mean ± SEM ($n = 6$ independent experiments). **(D)**: TCF7L2 expression was visualized by immunohistochemistry on sections from two independent fetal livers and adult livers. **(E)**: TCF7L2 expression was visualized by immunofluorescence on sections from fetal, neonatal, and adult livers. Nuclei were stained with 4′,6-diamidino-2-phenylindole (DAPI). **(F)**: TCF7L2 and TOM20 were analyzed by immunofluorescence on sections from neonatal livers. Nuclei were stained with DAPI. Arrows indicate cells with large mitochondrial networks and no expression of TCF7L2. **(G–J)**: Cells were transduced with non-target control shRNA (white bars) or specific shRNA against TCF7L2 (shTCF7L2) (grey bars). (G): mRNA abundance of TCF7L2 and PGC-1α. (H, I): Abundance of proteins analyzed by Western blot and quantification of the signal intensity. (J): Basal respiration determined by an extracellular flux analyzer. (G–J): Data are presented as mean ± SEM of $n = 7$ independent experiments. * or #, $p < .05$; ** or ##, $p < .01$; *** or ###, $p < .001$. For (C), *, comparisons versus day 0; #, comparisons between Diff and Undiff. Abbreviations: CV, central vein; OCR, oxygen consumption rate; PGC-1α, peroxisome proliferator-activated receptor gamma coactivator-1 alpha; PV, portal vein; shNT, non-target control shRNA.

OXPHOS. TCF7L2 is strongly repressed during the first days of the hepatocytic differentiation process, suggesting that its repression would be particularly important to initiate the induction of PGC-1α expression. PGC-1α is known to control its own expression in an auto-regulated manner [5], which may explain its sustained induction throughout the differentiation process, despite a weaker repression of TCF7L2 at later stages. Interestingly, previous data support a role for the downregulation of the Wnt/ß-catenin signaling pathway both in vivo [28], for the early stages of liver development and in vitro, for the hepatocytic differentiation of MSCs [33]. In umbilical cord blood-derived MSCs, the downregulation of *FRIZZLED 8*, a key component of the Wnt/β-catenin signaling pathway, was demonstrated to reduce TCF7L2 expression and favor the expression of several hepatocytic markers, including albumin, C/EBPα, and CYP1A1/2 [33]. While it was previously unclear how the downregulation of Wnt/β-catenin and TCF7L2 might contribute to the differentiation of hepatocytes, our data support the hypothesis that the TCF7L2-mediated control of PGC-1α expression, mitochondrial biogenesis and activity, are at least partly involved. Importantly, the activation of canonical Wnt signaling was reported to inhibit PGC-1α expression and the differentiation of brown adipocytes [34], suggesting that the Wnt/β-catenin-PGC-1α axis might connect mitochondrial biogenesis with stem cell differentiation into different lineages.

Conclusion

Although mitochondria and metabolism are now considered as critical regulators of the pluripotency and differentiation of stem cells [1, 29], the molecular mechanisms regulating the crosstalk between these two processes remain elusive. In this study, we provided data supporting that *TCF7L2* repression upon commitment to hepatocytic differentiation de-represses mitochondrial biogenesis and triggers the differentiation-associated metabolic shift toward OXPHOS, by inducing *PGC-1α* expression. In turn, PGC-1α and OXPHOS activity further contribute to the differentiation to the hepatocytic lineage, by regulating the expression of hepatocytic genes and supporting the morphological maturation associated with the differentiation process.

Importantly, better deciphering the interplay between mitochondria and stem cell differentiation should improve our ability to manipulate stem cells in vitro, which is of great interest for the development and optimization of stem cell-based therapeutics. In addition, since mitochondria regulate the pluripotency and function of stem cells, which are compromised upon aging and diseases, understanding this interplay might also lead to the development of regenerative medicine and novel anti-aging therapies.

Acknowledgments

We thank Pr. Sonveaux group (FATH, IREC, Université Catholique de Louvain, Belgium) for their help with respiration analyses, members of Dr N. Tiffin's group and SANBI (SANBI, University of the Western Cape, South Africa) for their warm welcome and helpful advice with bioinformatics analyses, and E. Di Valentin (University of Liège, Belgium) for his help with lentiviral vectors. This work was supported by fellowship from (Fonds National de la Recherche Scientifique [FNRS], Belgium) (to A.W.) and (Fonds de la Recherche dans l'Industrie et l'Agriculture [FRIA]) (to M.C.).

Author Contributions

A.W.: conceived and designed the study, performed experiments and collected data, analyzed and interpreted the data, wrote the manuscript; M.C.: performed experiments and collected data, analyzed and interpreted the data; J.-B.D.E., A.F., C.D., J.E., and H.E.-K.: performed experiments and collected data; M.N., G.P., and E.S.: provided administrative support and study material; T.A. and N.T.: analyzed and interpreted the data, provided administrative support and study material; M.N.: conceived and designed the study, analyzed and interpreted the data, provided administrative support and study material; P.R.: conceived and designed the study, analyzed and interpreted the data, wrote the manuscript, provided administrative support and study material.

Disclosure of Potential Conflicts of Interest

The authors indicated no potential conflicts of interest.

References

1 Xu X, Duan S, Yi F et al. Mitochondrial regulation in pluripotent stem cells. Cell Metabol 2013;18:325–332.

2 Mandal S, Lindgren AG, Srivastava AS et al. Mitochondrial function controls proliferation and early differentiation potential of embryonic stem cells. Stem Cells 2011;29:486–495.

3 Varum S, Momcilovic O, Castro C et al. Enhancement of human embryonic stem cell pluripotency through inhibition of the mitochondrial respiratory chain. Stem Cell Res 2009;3:142–156.

4 Mahato B, Home P, Rajendran G et al. Regulation of mitochondrial function and cellular energy metabolism by protein kinase C-lambda/tau: A novel mode of balancing pluripotency. Stem Cells 2014;32:2880–2892.

5 Hock MB, Kralli A. Transcriptional control of mitochondrial biogenesis and function. Ann Rev Physiol 2009;71:177–203.

6 Scarpulla RC, Vega RB, Kelly DP. Transcriptional integration of mitochondrial biogenesis. Trend Endocrinol Metabol 2012;23:459–466.

7 Tormos KV, Anso E, Hamanaka RB et al. Mitochondrial complex III ROS regulate adipocyte differentiation. Cell Metabol 2011;14:537–544.

8 Najar M, Raicevic G, Fayyad-Kazan H et al. Impact of different mesenchymal stromal cell types on T-cell activation, proliferation and migration. Int Immunopharmacol 2013;15:693–702.

9 Wang L, Feng Z, Wang X et al. DEGseq: An R package for identifying differentially expressed genes from RNA-seq data. Bioinformatics 2010;26:136–138.

10 Edgar R, Domrachev M, Lash AE. Gene Expression Omnibus: NCBI gene expression and hybridization array data repository. Nucleic Acids Res 2002;30:207–210.

11 Huang DW, Sherman BT, Lempicki RA. Bioinformatics enrichment tools: Paths toward the comprehensive functional analysis of large gene lists. Nucleic Acids Res 2009;37:1–13.

12 Wanet A, Remacle N, Najar M et al. Mitochondrial remodeling in hepatic differentiation and dedifferentiation. Int J Biochem Cell Biol 2014;54C:174–185.

13 Brand MD, Nicholls DG. Assessing mitochondrial dysfunction in cells. Biochem J 2011;435:297–312.

14 Chen CT, Shih YR, Kuo TK et al. Coordinated changes of mitochondrial biogenesis and antioxidant enzymes during osteogenic differentiation of human mesenchymal stem cells. Stem Cells 2008;26:960–968.

15 Fabregat I, Moreno-Caceres J, Sanchez A et al. TGF-beta signalling and liver disease. FEBS J 2016;283:2219–2232.
16 Palomaki S, Pietila M, Laitinen S et al. HIF-1alpha is upregulated in human mesenchymal stem cells. Stem Cells 2013;31:1902–1909.
17 Vega RB, Huss JM, Kelly DP. The coactivator PGC-1 cooperates with peroxisome proliferator-activated receptor alpha in transcriptional control of nuclear genes encoding mitochondrial fatty acid oxidation enzymes. Mol Cell Biol 2000;20:1868–1876.
18 Puigserver P, Wu Z, Park CW et al. A cold-inducible coactivator of nuclear receptors linked to adaptive thermogenesis. Cell 1998;92:829–839.
19 Rhee J, Inoue Y, Yoon JC et al. Regulation of hepatic fasting response by PPARgamma coactivator-1alpha (PGC-1): Requirement for hepatocyte nuclear factor 4alpha in gluconeogenesis. Proc Natl Acad Sci USA 2003;100:4012–4017.
20 Campbell CT, Kolesar JE, Kaufman BA. Mitochondrial transcription factor A regulates mitochondrial transcription initiation, DNA packaging, and genome copy number. Biochim Biophys Acta 2012;1819:921–929.
21 Clay Montier LL, Deng JJ Bai Y. Number matters: Control of mammalian mitochondrial DNA copy number. J Genet Genom 2009;36:125–131.
22 Nagaoka M, Duncan SA. Transcriptional control of hepatocyte differentiation. Prog Mol Biol Transl Sci 2010;97:79–101.
23 Charos AE, Reed BD, Raha D et al. A highly integrated and complex PPARGC1A transcription factor binding network in HepG2 cells. Genome Res 2012;22:1668–1679.
24 Puigserver P, Rhee J, Donovan J et al. Insulin-regulated hepatic gluconeogenesis through FOXO1-PGC-1alpha interaction. Nature 2003;423:550–555.
25 Knutti D, Kaul A, Kralli A. A tissue-specific coactivator of steroid receptors, identified in a functional genetic screen. Mol Cell Biol 2000;20:2411–2422.
26 Shitashige M, Hirohashi S, Yamada T. Wnt signaling inside the nucleus. Cancer Sci 2008;99:631–637.
27 Dowell KG, Simons AK, Bai H et al. Novel insights into embryonic stem cell self-renewal revealed through comparative human and mouse systems biology networks. Stem Cells 2014;32:1161–1172.
28 McLin VA, Rankin SA, Zorn AM. Repression of Wnt/beta-catenin signaling in the anterior endoderm is essential for liver and pancreas development. Development 2007;134:2207–2217.
29 Chen CT, Hsu SH, Wei YH. Mitochondrial bioenergetic function and metabolic plasticity in stem cell differentiation and cellular reprogramming. Biochim Biophys Acta 2012;1820:571–576.
30 Kawakami Y, Tsuda M, Takahashi S et al. Transcriptional coactivator PGC-1alpha regulates chondrogenesis via association with Sox9. Proc Natl Acad Sci USA 2005;102:2414–2419.
31 Lustig Y, Ruas JL, Estall JL et al. Separation of the gluconeogenic and mitochondrial functions of PGC-1{alpha} through S6 kinase. Genes Dev 2011;25:1232–1244.
32 Fernandez-Marcos PJ, Auwerx J. Regulation of PGC-1alpha, a nodal regulator of mitochondrial biogenesis. Am J Clin Nutr 2011;93:884S–8890.
33 Yoshida Y, Shimomura T, Sakabe T et al. A role of Wnt/beta-catenin signals in hepatic fate specification of human umbilical cord blood-derived mesenchymal stem cells. Am J Physiol Gastroint Liver Physiol 2007;293:G1089–G1098.
34 Kang S, Bajnok L, Longo KA et al. Effects of Wnt signaling on brown adipocyte differentiation and metabolism mediated by PGC-1alpha. Mol Cell Biol 2005;25:1272–1282.


See www.StemCells.com for supporting information available online.